Atmospheric Environment 92 (2014) 484–492

Contents lists available at ScienceDirect

Atmospheric Environment

journal homepage: www.elsevier.com/locate/atmosenv

Sources of polycyclic aromatic hydrocarbons in PM2.5 over the East China Sea, a downwind domain of East Asian continental outflow

Fengwen Wang [a], Tian Lin [b], Yuanyuan Li [a], Tianyi Ji [a], Chuanliang Ma [a], Zhigang Guo [a,*]

[a] Shanghai Key Laboratory of Atmospheric Particle Pollution and Prevention, Center for Atmospheric Chemistry Study, Department of Environmental Science and Engineering, Fudan University, 220 Handan Road, Shanghai 200433, China
[b] State Key Laboratory of Environmental Geochemistry, Institute of Geochemistry, Chinese Academy of Sciences, Guiyang 550002, China

HIGHLIGHTS

- A strong seasonal variation of 16 PAHs in PM2.5 over ECS was observed.
- Five sources of PAHs in PM2.5 over ECS were apportioned using PMF.
- The Asian continental outflow plays a key role on the PAHs in PM2.5 over ECS.
- Air–sea exchange was a potential source for LMW PAHs in PM2.5 over ECS.

ARTICLE INFO

Article history:
Received 23 January 2014
Received in revised form
28 April 2014
Accepted 1 May 2014
Available online 4 May 2014

Keywords:
Sources
PAHs
PMF
East Asian continental outflow
The East China Sea

ABSTRACT

A receptor site in the East China Sea (ECS), ~66 km off the shore of Shanghai, was used to investigate the seasonally atmospheric transport of land-based PAHs. Positive matrix factorization (PMF) modeling and back trajectories were performed to apportion the sources of the 16 USEPA priority PAHs (16 PAHs). In the process, three episodes were observed in all seasons except summer. These episodes provided additional insight to the transport mechanisms of these air pollutants in this most developed region of China. The average concentrations (in ng/m^3) of PAHs in PM2.5 in fall, winter, spring and summer were 5.26 ± 5.36, 10.41 ± 8.58, 3.93 ± 2.31 and 0.97 ± 0.25, respectively, and with an annual average of 5.24 ± 5.81. Low molecular weight (LMW) PAHs (i.e., 2 ~ 3-ring) was a dominant contributor for the 16 PAHs in PM2.5 over the ECS (36.2%), especially in summer (55.6%). The source apportionment by PMF analysis indicated that, based on yearly average, vehicular emission (27.0%) and coal combustion (24.5%) were the two major sources of PAHs, followed by biomass burning (16.5%), petroleum residue (16.3%) and air–surface exchange (15.7%). The highest source contributor for PAHs in fall and winter was coal combustion (30.5%) and vehicular emission (34.5%), respectively; while in spring and summer, the air–surface exchange contributed the most (27.1% and 59.5%, respectively). The specific composition patterns of 16 PAHs and PMF modeling results manifested that the air–sea exchange could be a potential source for the LMW PAHs in PM2.5 over the ECS, especially in warm season.

1. Introduction

Polycyclic aromatic hydrocarbons (PAHs) are a family of organic compounds that consist of fused aromatic rings. They are originated mainly from pyrogenic processes such as domestic and industrial coal combustion, biomass burning and vehicle emission (Harrison et al., 1996; Lima et al., 2005). PAHs are potentially carcinogenic or mutagenic and are associated with fine particles (i.e., PM2.5: aerodynamic diameter < 2.5 μm), therefore, they can be transported in the atmosphere to remote regions as far as the Arctic (Sofowote et al., 2011) and Antarctica (Masclet and Hoyau, 1994). This makes PAHs potentially important in the marine biogeochemical cycle and budget.

The ECS, a marginal sea off east China, is adjacent to the Yangtze River Delta (YRD). The YRD, covering 1.1% of the area of China (about 99,600 km^2), is the home to 108 million people (8.1% of the total population of China). The GDP of the YRD was 8214 billion yuan (renminbi, Chinese currency unit) in 2011, which represents 17.4% of the entire Chinese economy (www.hktdc.com). Shanghai, the biggest city in China, is the center of economy and

* Corresponding author.
E-mail address: guozgg@fudan.edu.cn (Z. Guo).

http://dx.doi.org/10.1016/j.atmosenv.2014.05.003
1352-2310/

manufacturing (light and heavy industry) of China. The circulation pattern of this region is influenced by the East Asian Monsoon, making the ECS as a downwind region of the Asian continental outflow and a sink of the pollutants transported not only from the YRD but also from North China (Lin et al., 2011; Zhang and Gao, 2007). Studying the contribution of anthropogenic pollutants in the ECS would provide useful information on these pollutants at the sources.

The outflow of the East Asian continental pollutants (crustal materials, dust, organic and elemental carbon, etc.) to the Bohai Sea, Yellow Sea, ECS, and northwest Pacific Ocean has been investigated (Duce et al., 1980; Gao et al., 1997; Hsu et al., 2009; Huebert et al., 2004). There also have been studies conducted on islands to investigate the pollutants transported from the land: Little Wheat Island (Gao et al., 1996), Tokchok Island (Lee et al., 2002), Gosan Island of Korea (Lee et al., 2006) in the Yellow Sea, and Cheju Island (Chen et al., 1997) and Amami and Miyako Islands around the ECS (Kaneyasu and Takada, 2004). The characteristics and sources of the carbonaceous components and ions in the aerosols at Changdao Island, located at the demarcation line between the Bohai Sea and Yellow Sea, were analyzed (Feng et al., 2007, 2012). However, there has been no report on the occurrence and sources of organic pollutants, such as PAHs in fine particles in atmosphere in the ECS. In this study, 80 seasonal PM2.5 samples were collected at a remotely small island in the ECS from October 2011 to August 2012. The objectives of this work are to examine the seasonal variation of the PAH concentration and composition, and to apportion the sources and contributions of the PAHs using positive matrix factorization (PMF), a receptor modeling.

2. Materials and methods

2.1. Sampling site and sample collection

The PM2.5 samples were collected at Huaniao Island (N30.86°, E122.67°) in the ECS approximately 66 km east to the shore off Shanghai (Fig. 1). Driven by the East Asian monsoon, the wind pattern arriving at Huaniao Island is mostly from west to east and north to south. This makes the island as an ideal observation site to assess the continental outflow to the northwest Pacific Ocean. To minimize the influence of local anthropogenic emissions, the sampling apparatus was placed on the rooftop of a three-story building (about 50 m above sea level) on the northwest side of the island, about 2 km from the population center. The permanent population on Huaniao Island is less than 1000 and there is almost no industry. Children and elderly people account for 80% of the total population. Most of the population is concentrated on the southeast of the island where a wharf is situated. There are only two automobiles on the island for delivery and passengers. Liquefied natural gas is used for cooking and the residents favor seafood best prepared by steaming or boiling. Biomass burning is controlled by the local government. This suggests that the PAH emissions from local anthropogenic activities is very low when compared with those transported from the mainland.

Quartz filters (20 × 25 cm^2, 2600QAT, PALL, USA) were used to collect PM2.5 samples by a PM2.5 sampler (Guangzhou Mingye Huanbao Technology Company) at a flow rate of ~335 m^3/day (Li et al., 2006). Sampler began to collect sample at 9:00 am on day one and stopped at 8:30 am on the next day, ensuring the duration time for a sample was about 23.5 h. About 20 samples were obtained in each season. A total of 80 PM2.5 samples were collected from October 23, 2011 to August 20, 2012. Two parallel operational sample blanks were obtained in each season. Before collecting the samples, the filters were wrapped in aluminum foil and baked together at 450 °C for 4 h to remove the residual organic contaminants.

2.2. Analytical procedures

The PAH analytical procedure and quality assurance/quality control (QA/QC) followed that described elsewhere (Mai et al., 2003; Guo et al., 2009). Briefly, prior to Soxhlet extraction a mixture of deuterated compounds including naphthalene (Nap-d_8, m/z 136), acenaphthene (Ace-d_{10}, m/z 164), phenanthrene (Phe-d_{10}, m/z 188), chryene (Chr-d_{12}, m/z 240) and perylene (Per-d_{12}, m/z 264) was added to all samples for the determination of the recovery rate. The Soxhlet extraction was for 48 h using dichloromethane (DCM) as the extracting solvent. The sample extracts were concentrated to about 5 ml using a vacuum rotary evaporator. Hexane (HEX) was used and the extracts were further concentrated to approximately 2 ml. All samples were then transferred into 22 ml glass cylinder tubes and concentrated to about 1 ml under gentle N_2 stream. The N_2 had a purity of 99%. The concentrated extracts were sequentially purified in the chromatography column filled with 3 cm deactivated alumina (Al_2O_3), 3 cm silica gel (SiO_2) and 1 cm anhydrous sodium sulfate (Na_2SO_4) and eluted with 20 ml of DCM/HEX (1:1, v: v). Prior to analysis for PAHs, the extracts were reduced to about 500 μL under a stream of purified N_2. Sample vial (2 ml) was prepared for the final concentrated extract and hexamethylbenzene (HMB) was used as internal standard to quantify the 16 PAHs. GC–MS analysis: all samples were injected with HMB, and then concentrated to about 200 μL preparing for GC–MS analysis. The GC-MSD (Agilent GC 6890 N coupled with 5975C MSD, equipped with DB5-MS column, 30 m × 0.25 mm × 0.25 μm) had helium as carrier gas. The GC operating processing was: held at 60 °C for 2 min, ramped to 290 °C at 3 °C/min and held for 20 min. The sample was injected split-less with the injector temperature at 290 °C. The post-run time was 5 min with oven temperature at 310 °C. The standard samples of 16 USEPA priority PAHs (16 PAHs) and 5 deuterated PAHs were purchased from Accu Standard, Inc. (USA). 16 targeted PAHs are as follows: 2-ring: naphthalene (Nap); 3-ring: acenaphthylene (Ac), acenaphthene (Ace), fluorene (Fl), phenanthrene (Phe), anthracene (Ant); 4-ring: fluoranthene (Flu), pyrene (Pyr), benzo[a]anthracene (BaA), chrysene (Chr); 5-ring: benzo[b]fluoranthene (BbF), benzo[k]fluoranthene (BkF), benzo[a]pyrene (BaP), dibenzo[a,h]anthracene (DBA); 6-ring: indeno[1,2,3-cd]pyrene (IP), benzo[ghi]perylene (BghiP).

2.3. QA/QC

Organic reagents (DCM, HMX) used in laboratory were purchased from Shanghai ANPEL Scientific Instrument Company (HPLC grade, purity: 95%). All vessels were firstly rinsed with hot potassium dichromate-sulfuric acid lotion, then laid for overnight and washed using 18.2 Ω Milli-Q water. After packing these vessels with aluminum foil, they were put in muffle furnace at 450 °C for 4 h. All utensils would be rinsed twice with reagents before used. Nominal detection limits for individual PAHs ranged from 0.008 to 0.08 ng/m^3 (Mai et al., 2003). The targeted 16 PAHs compounds were not detected in the procedural blank; the PAH recoveries of the standard-spiked matrix ranged from 85% to 95%; and the paired duplicate samples agreed to within 15% of the measured values (n = 10). The average surrogate recoveries were 69% ± 13% for Nap-d_8, 75% ± 16% for Ace-d_{10}, 90% ± 13% for Phe-d_{10}, 105% ± 10% for Chr-d_{12} and 103% ± 12% for Per-d_{12}, respectively. Sample results were displayed as blank correction by subtracting an average blank from each sample. Reported concentrations here were not recovery corrected.

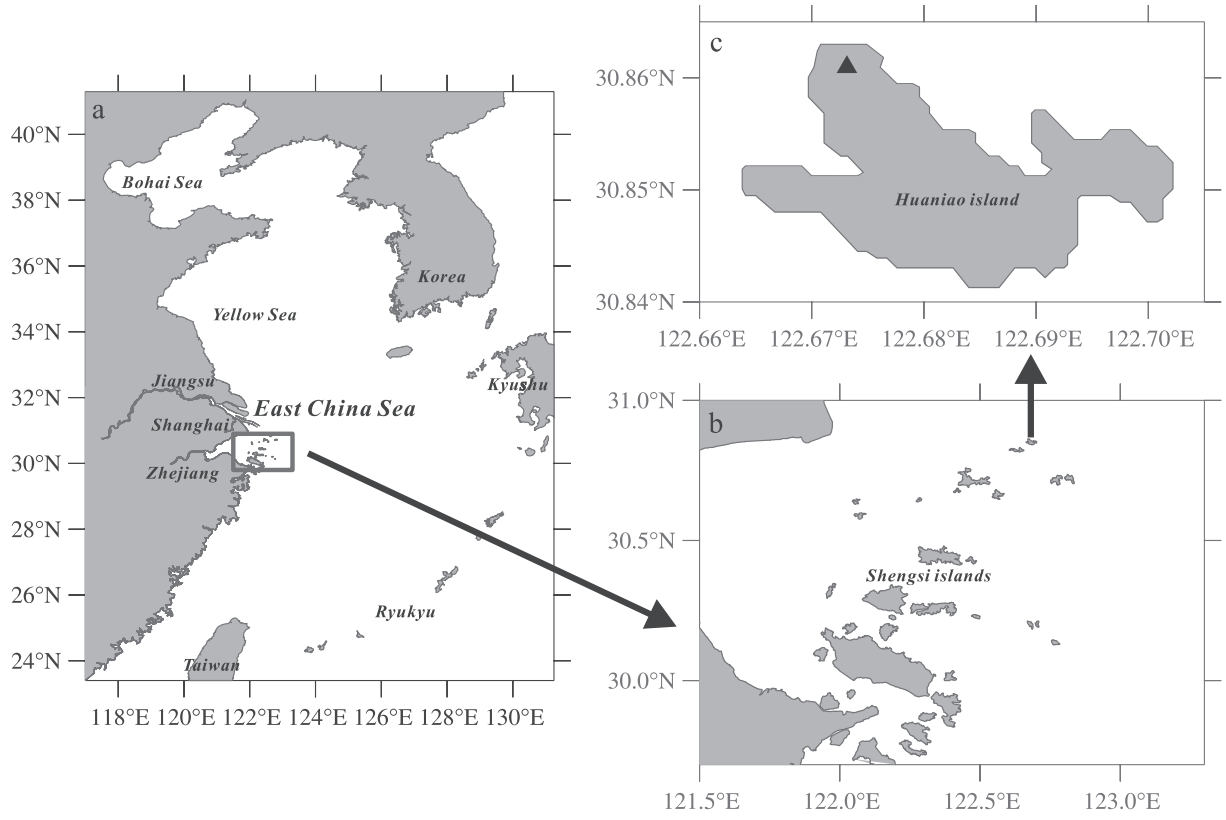

Fig. 1. Sampling site in the ECS.

2.4. PMF modeling

Detailed descriptions of PMF modeling application on source apportionment can be seen at EPA PMF 3.0 Fundamentals & User Guide (www.epa.gov/heasd/products/pmf). In brief, the PMF model is based on the following equation:

$$Xij = \sum_{k=1}^{p} AikFkj + Rij$$

where X_{ij} is the concentration of the j_{th} congener in the i_{th} sample of the original data set; A_{ik} is the contribution of the k_{th} factor to the i_{th} sample; F_{kj} is the fraction of the k_{th} factor arising from congener j; and R_{ij} is the residual between the measured X_{ij} and the estimated X_{ij} using p principal components.

$$Q = \sum_{i=1}^{n}\sum_{j=1}^{m}\left(\frac{Xij - \sum_{k=1}^{p} AikFkj}{Sij}\right)^2$$

where S_{ij} is the uncertainty of the j_{th} congener in the i_{th} sample of the original data set containing m congeners and n samples. Q is the weighted sum of squares of differences between the PMF output and the original data set. One of the objectives of PMF analysis is to minimize the Q value.

Importantly, there is a critical step in PMF analysis to determine the number of factors. Too few factors may not separate sources well, whereas too many factors may split a true source into two or more non-existing sources. Therefore, the frequency distributions of the scaled residuals as well as changes in the Q value must be a minimum or stable. This kind of method of determining the number of factors was described previously (Lee et al., 1999; Lin et al., 2011). In this study, the number of factors from 3 to 7 was examined with the optimal number of factors determined from the slope of the Q value versus the number of factors. For each run, the stability and reliability of the output were checked based on the Q value, residual analysis and correlation coefficients between observed and predicted concentrations. Finally, a 5-factor solution, which gave the most stable results and easily interpretable factors when taking the background of the PAH emission sources in China into consideration (Xu et al., 2006), was chosen for the data sets. Before the analysis, a data set including unique uncertainty values of each data point was created and inserted into the model. An uncertainty of 20% for each PAHs data set was used based on the results from regularly analyzing the standard reference material according to Mai et al., (2003).

2.5. Air mass back trajectory analysis

Air mass back trajectory was used to trace atmospheric transport path in this study. 3-day back trajectories at Huaniao Island at 1200 UTC were calculated at 700 m above ground level at 12-h intervals for the sampling days. HYSPLIT Trajectory Model from the National Oceanic and Atmospheric Administration (NOAA) (http://ready.arl.noaa.gov/hysplit-bin/trajasrc.pl) was used as the database. The integrated air masses were compiled by ArcGIS 9.3 (http://www.esri.com/).

3. Results and discussion

3.1. Occurrence of PAHs

The seasonal variation of the concentrations of 16 USEPA priority PAHs (16 PAHs) in the PM2.5 samples (histogram) and the ambient temperatures (solid line) at Huaniao Island in the ECS are

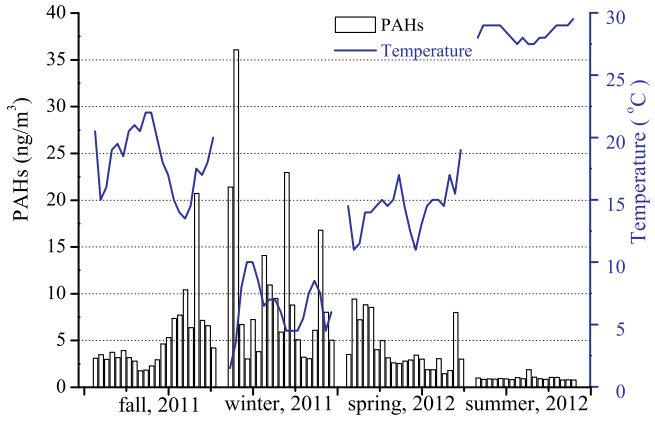

Fig. 2. Concentrations of 16 PAHs (histogram) and ambient temperature (solid line) at Huaniao Island in the ECS.

shown in Fig. 2. The concentrations of the individual PAHs are in Table S1. The concentrations of the 16 PAHs ranged from 0.78 to 36.08 ng/m^3 (average: 5.24 ± 5.81 ng/m^3). Table 1 showed that the mean concentration at Huaniao Island was lower than the other two receptor sites in China by a factor of 2–5 (Feng et al., 2007; Zhu et al., 2014). However, compared to those studies around the world, such as Lake Superior (Baker and Eisenreich, 1990), Amami and Miyako Islands (Kaneyasu and Takada, 2004), Haven Beach in Chesapeake Bay (Gustafson and Dickhut, 1997), Petrana in Western Greece (Terzi and Samara, 2004), and Mediterranean and Black Seas (Castro-Jiménez et al., 2012), the concentrations of PAHs in PM2.5 at Huaniao Island of the ECS were much higher.

A strong seasonal variation of the 16 PAH concentrations was observed (Fig. 2) with the highest in winter (10.41 ± 8.58 ng/m^3) and lowest in summer (0.97 ± 0.25 ng/m^3), and intermediates in fall and spring, 5.26 ± 5.36 ng/m^3 and 3.93 ± 2.31 ng/m^3, respectively. This seasonal trend was similar to the areas influenced by the Asian monsoon (Feng et al., 2007; Lee et al., 2006). The correlation between the PAH levels in the PM2.5 and ambient temperature was found to have a slightly negative correlation (R^2 = 0.33, n = 80). This indicates that ambient temperature may not be nearly as important as the other factors, such as emission sources and transport paths, on the PAH concentrations.

3.2. Compositions of PAHs

The 16 PAHs can be classified according to their properties and sources into 2 ~ 3-ring (Nap, Ac, Ace, Fl, Phe, Ant), 4-ring (Flu, Pyr, BaA, Chr), and 5 ~ 6-ring (BbF, BkF, BaP, IP, DBA, BghiP) PAHs. The seasonal variations of the 3 group contributions at Huaniao Island and Shanghai are shown in Fig. 3. The PM2.5 samples from Shanghai and Huaniao Island were simultaneously collected. A distinctly different composition pattern between the two sampling sites can be observed. Over the four seasons at Huaniao Island, the 2 ~ 3-ring PAHs contributed the most (36.2%), followed by the 5 ~ 6-ring (33.5%) and the 4-ring (30.3%). In Shanghai, however, the 5 ~ 6-ring contributed the most (56.5%), followed by 4 ~ ring (31.0%) and 2 ~ 3-ring (12.4%). It can also be seen that the 2 ~ 3-ring PAHs at Huaniao Island had the most pronounced seasonal variation. In fall and winter, the 2 ~ 3-PAHs contributed 24.9% and 22.2% of the 16 PAHs, respectively; while in spring and summer, the contributions increased notably and were as highly as 41.9% and 55.6%, respectively (Fig. 3a). The high contribution of the 2 ~ 3-ring PAHs in spring and summer at the ECS were significantly different from those reported in the urban areas in China, such as Shanghai and Qingdao. As shown in Fig. 3b, the 2 ~ 3-ring PAHs only accounted for 8.1% in spring and 11.7% in summer of the 16 PAHs in Shanghai, respectively. In spring and summer in Qingdao, the 2 ~ 3-ring PAHs were found to contribute 8.1% of the 16 PAHs (Guo et al., 2009). These differences indicate that these 2 ~ 3-ring PAHs in PM2.5 over the ECS may be specific in sources. This will be further discussed below.

3.3. Source identification of PAHs using diagnostic ratios

The diagnostic ratio method has been widely used to identify and characterize PAH emission sources. The distributions of the homologues are strongly associated with the formation mechanisms of the carbonaceous aerosols (Kavouras et al., 2001). The four diagnostic ratios used were Phe/(Phe + Ant), Flu/(Flu + Pyr), BaA/(BaA + Chr) and IP/(IP + BghiP), and the results are in Table 2. Phe/(Phe + Ant) varied from 0.86 to 0.99, suggesting that coal combustion/biomass burning was the dominant source. Flu/(Flu + Pyr) in each season were 0.44–0.96, indicating a mixed contribution from the combustion of liquid fossil fuels as well as biomass and coal burning. BaA/(BaA + Chr) in all seasons were 0.29–0.57, characterizing petrogenic and pyrolytic origins. IP/(IP + BghiP) in fall were 0.45–0.58, implying a mixed sources of coal, biomass and fuel combustion. In winter, they were all above 0.5, indicating a strong contribution from coal and biomass combustion. In spring and summer, IP/(IP + BghiP) were less than 0.5, implying a main source from the fossil fuel combustion.

3.4. Source apportionment by PMF

PMF modeling, which quantitatively estimates the contributions from specific sources, has been widely used to apportion the sources of PAHs in aerosols on the basis of spatially distributed data sets. In this study, an 80 × 15 (80 samples with 15 PAHs each) data set was introduced to the EPA PMF 3.0 model to estimate the source contributions of the 16 PAHs. As DBA was under the detection limit in most of the samples, it was excluded from the analysis. After testing from 3 to 7 factors, a 5-factor solution was adopted.

Table 1
Comparison of atmospheric PAH concentrations in PM2.5 over the ECS with those in other regions in the world.

Location	Type of site	Description	Concentrations (ng/m^3)	Reference
East China Sea	Remote island	PM2.5	5.24 ± 5.81	This study
Yellow and Bohai Sea	Remote island	PM2.5	33.60 ± 39.21	Feng et al. (2007)
North China Plain	Background site	TSP	18.95 ± 16.51	Zhu et al. (2014)
Lake Superior	Remote island	TSP	0.12 ± 0.06	Baker and Eisenreich (1990)
Around East China Sea	Remote island	PM2.5	1.49 ± 0.43	Kaneyasu and Takada (2004)
Chesapeake Bay	Background site	TSP	0.005–0.50	Gustafson and Dickhut (1997)
Western Greece	Background site	TSP	0.8 ± 0.84	Terzi and Samara (2004)
Mediterranean and Black Seas	Cruise campaign	TSP	0.51–3.06 and 0.94–2.45	Castro-Jiménez et al. (2012)

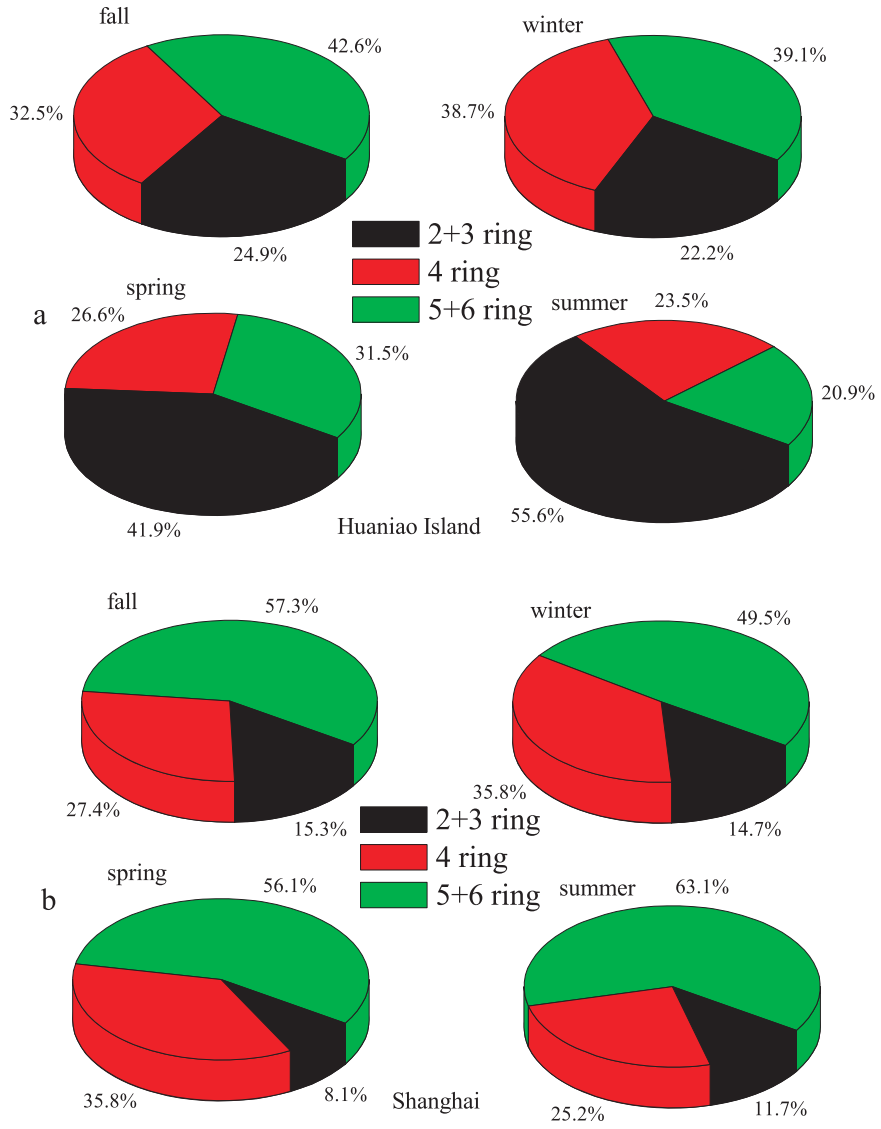

Fig. 3. Seasonal variations of relative compositions of 2 ~ 3-ring, 4-ring and 5 ~ 6-ring PAHs in PM2.5 at Huaniao Island in the ECS (a) and Shanghai (b).

Correlation indices between the estimated concentrations and the measured concentrations were between 0.58 (Nap) and 0.99 (Phe, Flu, BbF, BkF, IP and BghiP), suggesting that the measured concentrations were well explained by the 5 factors selected. 5 source contributions on whole samples and PMF factor profiles are shown in Fig. 4.

Factor 1 accounted for 24.5% of the sum of the measured 15 PAHs. It has high loadings of Flu and Pyr, and moderate contributions from Chr, BbF, BaP and BghiP. Flu and Pyr have been considered to be markers of coal combustion (Harrison et al., 1996). Coal combustion was estimated to contribute 20% of the total 16 PAH emissions in China in 2003 (Xu et al., 2006). According to NBSC (http://www.stats.gov.cn/english/), coal consumption in China accounted for more than 70% of the total energy used in 2011. The rapid industrialization of the coastal areas of China dramatically increased coal consumption in the past decades. Although the energy structure in northeast China has been shifting since the early 1990s from coal to oil and/or natural gas, and large-scale improvement of combustion facilities has been implemented, coal combustion is still an important source of PAHs in the aerosols and sediments (Lin et al., 2011; Ma et al., 2011).

Factor 2 contributed 27.0% of all the measured 15 PAHs. High loadings of BbF, IP and BghiP and moderate loadings of Flu, Pyr, BbA, Chr and BkF were observed. Similar profile of high loadings of IP and BghiP were also observed in the sediments from the Bohai and Yellow Sea (Lin et al., 2011). Hereby, factor 2 is characterized as vehicular emissions. The YRD, including the most developed regions in China (Jiangsu and Zhejiang provinces, and Shanghai), has been experiencing very rapid increase in vehicles, private or public. Shanghai had 3.10×10^6 vehicles in 2011, a significant source of vehicular emissions by any measure.

Factor 3 explained 16.5% of the sum of the measured 15 PAHs. It was dominated by Phe, Flu and BbF, with moderate loadings of Chr, BkF, BaA, IP and BghiP. Flu, BbF and BkF are three of the most abundant species in the burning of agricultural refuse which can also emit moderate amount of Phe, BaA, IP and BghiP (Rajput et al., 2011). In rural China, agricultural refuse or firewood are still the most important fuels used for cooking and space heating. They are often burned in primitive stoves without forced blast, emitting ample organic pollutants including PAHs.

Factor 4 accounted for 15.8% of all measured 15 PAHs. It was highly loaded with Nap, Ace, Fl, Phe, moderately with Flu, Pyr, Chr,

Table 2
Diagnostic ratios of PAH in PM2.5 in each season at Huaniao Island in the ECS.

	Phe/Phe + Ant	Flu/Flu + Pyr	BaA/BaA + Chr	IP/IP + BghiP
Fall	0.86–0.93	0.56–0.59	0.34–0.57	0.45–0.58
Winter	0.95–0.99	0.44–0.96	0.29–0.49	0.56–0.77
Spring	0.88–0.93	0.53–0.64	0.35–0.51	0.46–0.50
Summer	0.88–0.91	0.55–0.59	0.36–0.51	0.43–0.47
Diagnostic ratios	0.5 gasoline	<0.4 Unburned petroleum	<0.2 petrogenic	<0.5 engine fuel combustion
	0.65 diesel	0.4–0.5 liquid fossil fuel	0.2–0.35 petrogenic and combustion	
	0.76 coal	>0.5 wood, coal combustion	>0.35 pyrolytic sources	>0.5 coal/biomass combustion
References	Yunker et al., 2002	Yunker et al., 2002	Simcik et al., 1999	Yunker et al., 2002

and slightly with the 5 ~ 6-ring PAHs. This profile contains more volatile PAHs (i.e., 2 ~ 3-rings) and is readily found in summer. Nap has been used as a tracer of the fugitive loss of petroleum products (Khairy and Lohmann, 2013). Ace, Fl and Phe are abundant in natural mineral dust transport (Moon et al., 2008). Moreover, the low molecular weight (LMW) PAHs are favored in air–sea exchange (Cheng et al., 2012; Gigliotti et al., 2002). Other studies confirmed that the water column could contribute to the PAHs burden in the atmosphere, particularly in the summer months (Nelson et al., 1998). In addition, it has been suggested that soil could also be a potential source of PAHs in atmosphere driven by higher temperatures (Agarwal, 2009). LMW PAHs can be transported long distances and deposit on surfaces. Accordingly, factor 4 was attributed to air–surface exchange. Such kind of "air–surface exchange" was believed to contribute to 25% of the atmospheric PAHs (gas + particle) in the Hudson River Estuary Airshed (Lee et al., 2004). The "exchange" here indicates a possible re-emission of aged PAHs from "contaminated soil" or volatilization of PAHs directly from the water column of ECS into the atmosphere, to be absorbed later by the particles.

Factor 5 accounted for 16.3% of all the measured 15 PAHs. The profile was dominated by Phe and other 3 ~ 4-ring PAHs. This kind of profile has been suggested to be mainly from crude oil leakage or refined petroleum release (Zakaria et al., 2002). This source can be emissions due to fuel handling and/or refueling of ships in the ECS and leakage on land. Consequently, factor 5 was selected to represent petroleum residue source.

The seasonal contributions of each source to the 15 PAHs are in Fig. 5. A strong seasonal variation is observed: the highest contributor in fall was coal combustion (30.5%) and in winter it was vehicular emission (34.5%), while air–surface exchange was the main contributor in both spring (27.1%) and summer (59.5%). The wind direction in fall and winter at Huaniao Island was mostly from the west (Zhu et al., 2013), indicating a strong

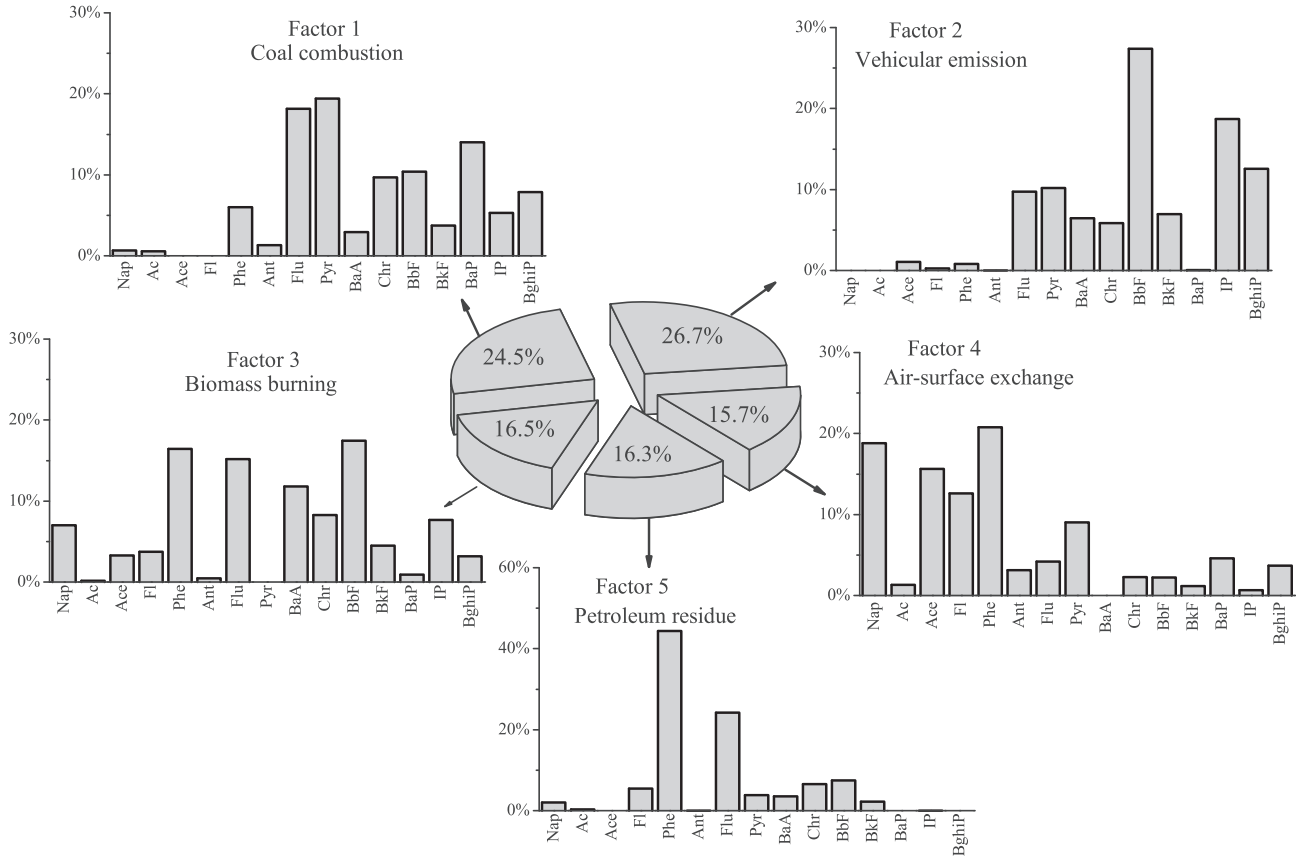

Fig. 4. 5-factor loadings by PMF analysis from 16 PAHs data of 80 PM2.5 samples collected at Huaniao Island in the ECS and the source contribution percentages.

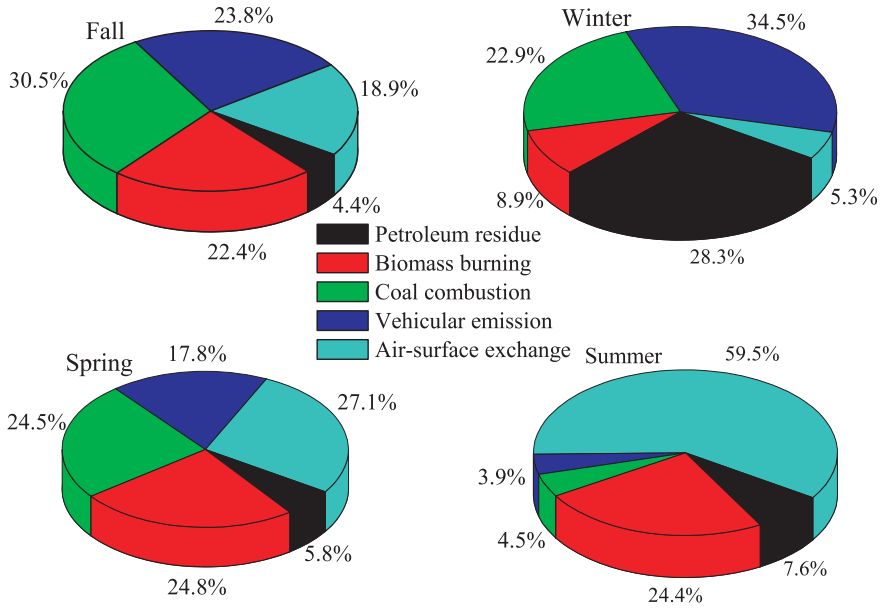

Fig. 5. Contributions of the five sources to 16 PAHs in PM2.5 over the ECS in four seasons.

influence of the continental outflow on this receptor site. The intense manufacturing activities of the YRD and North China demand large amount of energy provided mostly by coal-fired power plants, and the large vehicular fleet is the rapid growing source of emissions. Moreover, the contribution from petroleum residue (28.3%) in winter increased much more than that of fall (4.4%). Petroleum residue-derived PAHs mainly consist of the more volatile PAHs with 3 ~ 4-rings. These PAHs are readily partitioned to the particle phase at lower temperatures, leading to high PAHs in the PM2.5 in winter. In contrast, in the winter of Changdao Island and Qingdao, coal combustion was the larger contributor of PAHs in PM2.5 than vehicular emission (Lin et al., 2011), because of the space heating strategy or policy in North China. Technically, space heating is not allowed in the south in winter, while in the north, coal-fired centralized heating is provided. Air-surface and air-sea exchanges of LMW PAHs are temperature-sensitive processes and are both important in this study. Considering the high concentrations of the 2 ~ 3-ring PAHs in the PM2.5 as described above (Fig. 3a) and the southeasterly winds in the summer in the ECS, it is reasonable to infer that the air–sea exchange in the ECS could be a crucial contributor of these LMW PAHs in the PM2.5. The further study of air–sea exchange of PAHs in the water column and the gas phase would prove to be interesting and fruitful.

3.5. *Influence of long-range transport of air mass during episodes on the PAH levels*

Three-day air mass back trajectories at 700 m originating at Huaniao Island and the concentrations of the PAHs in the PM2.5 are in Fig. 6. It can be seen that most of the air parcels arriving at Huaniao Island in the summer were from the east (open sea); whereas in the winter they were transported from northern China. In spring and fall, the air masses were mostly from the land with some from the sea. Therefore, only in the summer the atmosphere over Huaniao Island is not mainly influenced by continental outflow. Three episodes were observed in each season except summer as designated by the red back trajectories and histograms in Fig. 6: (1) 11–13 Nov., 2011, (2) 24–25 Dec., 2011, and (3) 31 March and 3–5 April, 2012.

In the fall episode (11–13 Nov., 2011), the average concentration of the 16 PAHs was 12.49 ng/m^3 while the non-episodic average was only 4.87 ng/m^3. The 4 ~ 5-ring PAHs, such as Flu, BaA and BbF, increased dramatically during this episode. PMF results revealed that biomass burning PAHs were more than doubled (14.0% of the total PAHs in the non-episodic days and 30.0% in the episodic days). The fire map during this episode is shown in Fig. S1 (http://firms.modaps.eosdis.nasa.gov/firemap/). The red spots were the fire spots observed in the episode. It could be seen that the air masses passed over the fires before arriving at Huaniao Island. In addition, our yet to be published elemental data showed high K^+ in the PM2.5 during the episode, suggesting significant contribution from biomass burning (Feng et al., 2012).

In the winter episode (24–25 Dec., 2011), the average concentration of the 16 PAHs was at 28.74 ng/m^3; while for the non-episodic average it was only 8.25 ng/m^3, an over three-fold difference amid. Fossil fuel combustion-derived PAHs, such as Phe, Pyr, BbF and BaP, increased remarkably. Back trajectories suggested that the air masses were from northern China where coal-fired boiler and biomass were usually used for heating space in the winter (Tian et al., 2009; Zhang and Tao, 2008). PMF results showed that the contribution from coal combustion and biomass burning to the 16 PAHs increased from 22.0% in the non-episode to as high as 40.3% in this episode. Ambient temperature was extremely low in northern China (http://www.tianqihoubao.com/weather/city.aspx) and Huaniao Island (Fig. 2) in this episode. Therefore, the increasing emission levels of the PAHs during the episode could be attributed to intensive coal and biomass usage when the cold air stroke at northern China.

In the spring episode (31 March and 3–5 April, 2012), the average concentration of the 16 PAHs was 8.50 ng/m^3; while the non-episodic average was only 3.33 ng/m^3. PMF results showed that coal combustion (30.6%) and vehicular emissions (19.9%) contributed 50.5% of the total PAHs in the episode, while in the other days they only contributed 20.5% (11.4% for coal combustion and 9.1% for vehicular emissions). It can be seen that the air masses were from remote northern China where Asian dust storm events frequently occur during the spring season (Duce et al., 1980; Zhang and Gao, 2007) and they passed over eastern China where there are extensive anthropogenic activities. More importantly, our yet to be

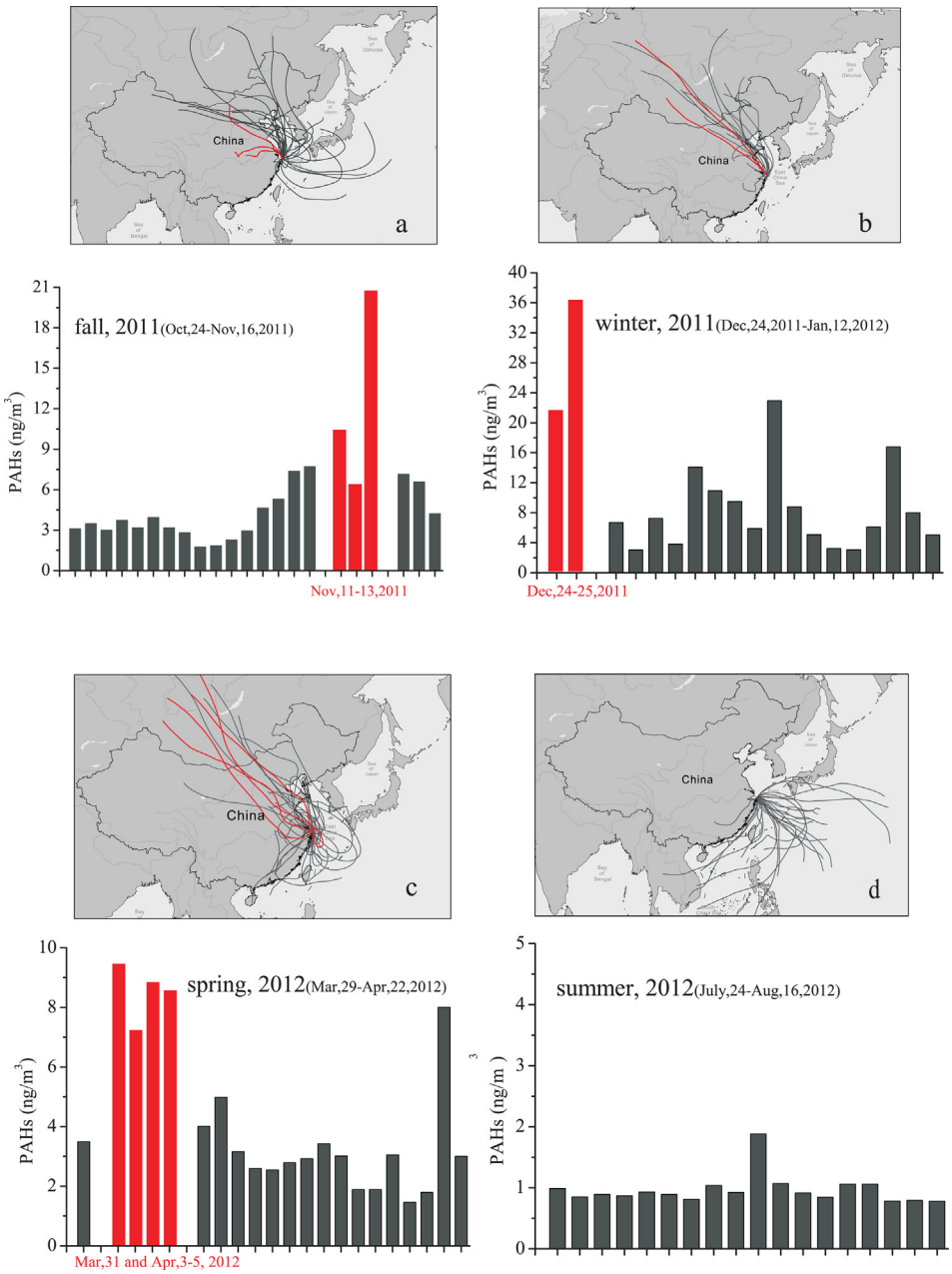

Fig. 6. Variation of PAHs concentrations in PM2.5 in four seasons and associated 3-days transport pathway of air masses arriving at Huaniao Island in the ECS.

published data about the concentrations of Ca and Al also increased notably during this episode, and the Ca/Al was 0.96–1.06, suggesting the mixing of transported mineral dust with local anthropogenic emissions (Yuan et al., 2008). This indicated that the high level of PAHs in this episode could be attributed to the contribution from the long-range transport of East Asian dusts mixed with anthropogenic pollutants in the transport path.

4. Conclusions

The annual average concentration of 16 PAHs in PM2.5 was 5.24 ± 5.81 ng/m^3. The seasonal composition pattern of the 16 PAHs in PM2.5 over the ECS was significantly different from those reported at urban areas in China. Diagnostic ratios revealed coal/biomass combustion and vehicular emission as the main sources of PAHs. PMF identified that the highest source contributor for PAHs in fall was coal combustion (30.5%) and in winter it was vehicular emission (34.5%); while in spring and summer it was air–surface exchange (27.1% and 59.5%, respectively). The results obtained by air mass back trajectory analysis and source apportionment using PMF complemented each other well, thus generating a more comprehensive understanding of the sources of PM2.5-bound PAHs in episodes over the ECS.

Acknowledgment

This work was supported by the National Natural Science Foundation of China (NSFC) (No: 41176085), National Basic Research Program of China (No: 2014CB953701) and Shanghai Science and Technology Committee (No: 12DJ1400102). We are most grateful to Prof. Ming Fang of the Hong Kong University of Science and Technology for his invaluable advices and comments.

We would like to thank Mr. Fujiang Wang for his help in sample collection. The anonymous reviewers should be sincerely appreciated for their constructive comments that greatly improved this study.

Appendix A. Supplementary data

Supplementary data related to this article can be found at http://dx.doi.org/10.1016/j.atmosenv.2014.05.003.

References

Agarwal, T., 2009. Concentration level, pattern and toxic potential of PAHs in traffic soil of Delhi, India. J. Hazard. Mater. 171, 894–900.

Baker, J., Eisenreich, S., 1990. Concentrations and fluxes of polycyclic aromatic hydrocarbons and polychlorinated biphenyls across the air-water interface of Lake Superior. Environ. Sci. Technol. 24, 342–352.

Castro-Jiménez, J., Berrojalbiz, N., Wollgast, J., Dachs, J., 2012. Polycyclic aromatic hydrocarbons (PAHs) in the Mediterranean Sea: atmospheric occurrence, deposition and decoupling with settling fluxes in the water column. Environ. Pollut. 166, 40–47.

Chen, L., Carmichael, G., Hong, M., Ueda, H., Shim, S., Song, C., Kim, Y., Arimoto, R., Prospero, J., Savoie, D., 1997. Influence of continental outflow events on the aerosol composition at Cheju Island, South Korea. J. Geophys. Res. 102, 28551–28574.

Cheng, J., Ko, F., Lee, C., Fang, M., 2012. Air-water exchange fluxes of polycyclic aromatic hydrocarbons in the tropical coast, Taiwan. Chemosphere 90, 2614–2622.

Duce, R., Unni, C., Ray, B., Prospero, J., Merrill, J., 1980. Long-range atmospheric transport of soil dust from Asia to the tropical North Pacific: temporal variability. Science 209, 1522.

Feng, J., Guo, Z., Chan, C., Fang, M., 2007. Properties of organic matter in $PM_{2.5}$ at Changdao Island, China–a rural site in the transport path of the Asian continental outflow. Atmos. Environ. 41, 1924–1935.

Feng, J., Guo, Z., Zhang, T., Yao, X., Chan, C., Fang, M., 2012. Source and formation of secondary particulate matter in $PM_{2.5}$ in Asian continental outflow. J. Geophys. Res. 117, D03302.

Gao, Y., Arimoto, R., Duce, R., Chen, L., Zhou, M., Gu, D., 1996. Atmospheric non-sea-salt sulfate, nitrate and methanesulfonate over the China Sea. J. Geophys. Res. Atmos. 101, 12601–12611.

Gao, Y., Arimoto, R., Duce, R., Zhang, X., Zhang, G., An, Z., Chen, L., Zhous, M., Gu, D., 1997. Temporal and spatial distributions of dust and its deposition to the China Sea. Tellus B 49, 172–189.

Gigliotti, C., Brunciak, P., Dachs, J., Glenn, I., Thomas, R., Nelson, E., Totten, L., Eisenreich, S., 2002. Air-water exchange of polycyclic aromatic hydrocarbons in the New York, New Jersey, USA, Harbor Estuary. Environ. Toxicol. Chem. 21, 235–244.

Guo, Z., Lin, T., Zhang, G., Hu, L., Zheng, M., 2009. Occurrence and sources of polycyclic aromatic hydrocarbons and n-alkanes in $PM_{2.5}$ in the roadside environment of a major city in China. J. Hazard. Mater. 170, 888–894.

Gustafson, K., Dickhut, R., 1997. Particle/gas concentrations and distributions of PAHs in the atmosphere of southern Chesapeake Bay. Environ. Sci. Technol. 31, 140–147.

Harrison, R., Smith, D., Luhana, L., 1996. Source apportionment of atmospheric polycyclic aromatic hydrocarbons collected from an urban location in Birmingham, UK. Environ. Sci. Technol. 30, 825–832.

Hsu, S., Liu, S., Arimoto, R., Liu, T., Huang, Y., Tsai, F., Lin, F., Kao, S., 2009. Dust deposition to the East China Sea and its biogeochemical implications. J. Geophys. Res. 114, D15304.

Huebert, B., Bertram, T., Kline, J., Howell, S., Eatough, D., Blomquist, B., 2004. Measurements of organic and elemental carbon in Asian outflow during ACE-Asia from the NSF/NCAR C-130. J. Geophys. Res. 109, D19S11.

Kaneyasu, N., Takada, H., 2004. Seasonal variations of sulfate, carbonaceous species (black carbon and polycyclic aromatic hydrocarbons), and trace elements in fine atmospheric aerosols collected at subtropical islands in the East China Sea. J. Geophys. Res. 109, D06211.

Kavouras, I., Koutrakis, P., Tsapakis, M., Lagoudaki, E., Stephanou, E., Von Baer, D., Oyola, P., 2001. Source apportionment of urban particulate aliphatic and polynuclear aromatic hydrocarbons (PAHs) using multivariate methods. Environ. Sci. Technol. 35, 2288–2294.

Khairy, M., Lohmann, R., 2013. Source apportionment and risk assessment of polycyclic aromatic hydrocarbons in the atmospheric environment of Alexandria, Egypt. Chemosphere 91, 895–903.

Lee, E., Chan, C., Paatero, P., 1999. Application of positive matrix factorization in source apportionment of particulate pollutants in Hong Kong. Atmos. Environ. 33, 3201–3212.

Lee, J., Gigliotti, C., Offenberg, J., Eisenreich, S., Turpin, B., 2004. Sources of polycyclic aromatic hydrocarbons to the Hudson River Airshed. Atmos. Environ. 38, 5971–5981.

Lee, J., Kim, Y., Kang, C., Ghim, Y., 2006. Seasonal trend of particulate PAHs at Gosan, a background site in Korea between 2001 and 2002 and major factors affecting their levels. Atmos. Res. 82, 680–687.

Lee, S., Bae, G., Moon, K., Pyo Kim, Y., 2002. Characteristics of TSP and $PM_{2.5}$ measured at Tokchok Island in the Yellow Sea. Atmos. Environ. 36, 5427–5435.

Li, J., Zhang, G., Li, X., Qi, S., Liu, G., Peng, X., 2006. Source seasonality of polycyclic aromatic hydrocarbons (PAHs) in a subtropical city, Guangzhou, South China. Sci. Total Environ. 355, 145–155.

Lima, A., Farrington, J., Reddy, C., 2005. Combustion-derived polycyclic aromatic hydrocarbons in the environment-a review. Environ. Forensics 6, 109–131.

Lin, T., Hu, L., Guo, Z., Qin, Y., Yang, Z., Zhang, G., Zheng, M., 2011. Sources of polycyclic aromatic hydrocarbons to sediments of the Bohai and Yellow Seas in East Asia. J. Geophys. Res. 116, D23305.

Ma, W., Sun, D., Shen, W., Yang, M., Qi, H., Liu, L., Shen, J., Li, Y., 2011. Atmospheric concentrations, sources and gas-particle partitioning of PAHs in Beijing after the 29th Olympic Games. Environ. Pollut. 159, 1794–1801.

Mai, B., Qi, S., Zeng, E., Yang, Q., Zhang, G., Fu, J., Sheng, G., Peng, P., Wang, Z., 2003. Distribution of polycyclic aromatic hydrocarbons in the coastal region off Macao, China: assessment of input sources and transport pathways using compositional analysis. Environ. Sci. Technol. 37, 4855–4863.

Masclet, P., Hoyau, V., 1994. Evidence for the presence of polycyclic aromatic hydrocarbons in the polar atmosphere and in polar ice: Ice archives in Antarctica and Greenland. Analusis 22, M31–M33.

Moon, K., Han, J., Ghim, Y., Kim, Y., 2008. Source apportionment of fine carbonaceous particles by positive matrix factorization at Gosan background site in East Asia. Environ. Int. 34, 654–664.

Nelson, E., McConnell, L., Baker, J., 1998. Diffusive exchange of gaseous polycyclic aromatic hydrocarbons and polychlorinated biphenyls across the air-water interface of the Chesapeake Bay. Environ. Sci. Technol. 32, 912–919.

Rajput, P., Sarin, M., Rengarajan, R., Singh, D., 2011. Atmospheric polycyclic aromatic hydrocarbons (PAHs) from post-harvest biomass burning emissions in the Indo-Gangetic Plain: Isomer ratios and temporal trends. Atmos. Environ. 45, 6732–6740.

Simcik, M., Eisenreich, S., Lioy, P., 1999. Source apportionment and source/sink relationships of PAHs in the coastal atmosphere of Chicago and Lake Michigan. Atmos. Environ. 33, 5071–5079.

Sofowote, U., Hung, H., Rastogi, A., Westgate, J., Deluca, P., Su, Y., McCarry, B., 2011. Assessing the long-range transport of PAH to a sub-Arctic site using positive matrix factorization and potential source contribution function. Atmos. Environ. 45, 967–976.

Terzi, E., Samara, C., 2004. Gas-particle partitioning of polycyclic aromatic hydrocarbons in urban, adjacent coastal, and continental background sites of western Greece. Environ. Sci. Technol. 38, 4973–4978.

Tian, F., Chen, J., Qiao, X., Wang, Z., Yang, P., Wang, D., Ge, L., 2009. Sources and seasonal variation of atmospheric polycyclic aromatic hydrocarbons in Dalian, China: factor analysis with non-negative constraints combined with local source fingerprints. Atmos. Environ. 43, 2747–2753.

Xu, S., Liu, W., Tao, S., 2006. Emission of polycyclic aromatic hydrocarbons in China. Environ. Sci. Technol. 40, 702–708.

Yuan, H., Zhuang, G., Li, J., Wang, Z., Li, J., 2008. Mixing of mineral with pollution aerosols in dust season in Beijing: revealed by source apportionment study. Atmos. Environ. 42, 2141–2157.

Yunker, M., Macdonald, R., Vingarzan, R., Mitchell, R., Goyette, D., Sylvestre, S., 2002. PAHs in the Fraser River basin: a critical appraisal of PAH ratios as indicators of PAH source and composition. Org. Geochem. 33, 489–515.

Zakaria, M., Takada, H., Tsutsumi, S., Ohno, K., Yamada, J., Kouno, E., Kumata, H., 2002. Distribution of polycyclic aromatic hydrocarbons (PAHs) in rivers and estuaries in Malaysia: a widespread input of petrogenic PAHs. Environ. Sci. Technol. 36, 1907–1918.

Zhang, K., Gao, H., 2007. The characteristics of Asian-dust storms during 2000–2002: from the source to the sea. Atmos. Environ. 41, 9136–9145.

Zhang, Y., Tao, S., 2008. Seasonal variation of polycyclic aromatic hydrocarbons (PAHs) emissions in China. Environ. Pollut. 156, 657–663.

Zhu, L., Chen, Y., Guo, L., Wang, F., 2013. Estimate of dry deposition fluxes of nutrients over the East China Sea: the implication of aerosol ammonium to non-sea-salt sulfate ratio to nutrient deposition of coastal oceans. Atmos. Environ. 69, 131–138.

Zhu, Y., Yang, L., Yuan, Q., Yan, C., Dong, C., Meng, C., Sui, X., Yao, L., Yang, F., Lu, Y., 2014. Airborne particulate polycyclic aromatic hydrocarbon (PAH) pollution in a background site in the North China Plain: concentration, size distribution, toxicity and sources. Sci. Total Environ. 466, 357–368.